


Phase behavior of hard circular arcs

Juan Pedro Ramírez González 

*Departamento de Física Teórica de la Materia Condensada, Universidad Autónoma de Madrid,
Ciudad Universitaria de Cantoblanco, 28049 Madrid, Spain*

Giorgio Cinacchi 

Departamento de Física Teórica de la Materia Condensada, Instituto de Física de la Materia Condensada (IFIMAC), Instituto de Ciencias de Materiales “Nicolás Cabrera”, Universidad Autónoma de Madrid, Ciudad Universitaria de Cantoblanco, 28049 Madrid, Spain



(Received 30 June 2021; accepted 12 October 2021; published 9 November 2021)

By using Monte Carlo numerical simulation, this work investigates the phase behavior of systems of hard infinitesimally thin circular arcs, from an aperture angle $\theta \rightarrow 0$ to an aperture angle $\theta \rightarrow 2\pi$, in the two-dimensional Euclidean space. Except in the isotropic phase at lower density and in the (quasi)nematic phase, in the other phases that form, including the isotropic phase at higher density, hard infinitesimally thin circular arcs autoassemble to form clusters. These clusters are either filamentous, for smaller values of θ , or roundish, for larger values of θ . Provided the density is sufficiently high, the filaments lengthen, merge, and straighten to finally produce a filamentary phase while the roundels compact and dispose themselves with their centers of mass at the sites of a triangular lattice to finally produce a cluster hexagonal phase.

DOI: [10.1103/PhysRevE.104.054604](https://doi.org/10.1103/PhysRevE.104.054604)

I. INTRODUCTION AND MOTIVATION

Many aspects of the physics of [(soft-)condensed] states of matter [1] can be fruitfully investigated by resorting to basic simple systems of hard particles [2]. Such particles interact between them solely via infinitely repulsive short-range interactions preventing them from intersecting. Thus, entropy is, on varying the number density ρ , the sole physical magnitude that determines the phase behavior of such systems. Yet the infinitely repulsive short-range interactions provenly suffice for causing multiple fluid and solid states of matter to occur in systems of particles interacting via them. This fact, together with their omnipresence across length scales, justifies the interest in systems of hard particles.

The hard sphere is basic to broad condensed matter and statistical physics. Systems of hard spheres have been extensively investigated with different composition and under a variety of conditions: A vast literature has been accumulated [2].

In the course of the past 50 years, the investigation has been progressively expanded to systems of hard nonspherical particles [2]. They form more complex instances of the fluid and solid states of matter that systems of hard spheres already exhibit [1,2] along with genuinely new plastic-crystalline [2,3] and liquid-crystalline [1,2,4–6] states of matter. The investigation on this progressively expanding variety of systems of hard nonspherical particles has actually shown how finely the hard-particle shape may determine the system phase behavior [2].

The majority of these hard nonspherical particles are convex [2]. If nonsphericity causes genuinely new states of matter to occur, nonconvexity might promote special instances of

fluid and solid states of matter. These states of matter might be difficult to achieve or entirely precluded in systems of hard convex (yet dexterously shaped) particles.

Out of the minority of hard concave particles that have been considered thus far [7], one is the hard spherical cap(sid) [8]. It consists of that portion of a spherical surface in the three-dimensional Euclidean space \mathbb{R}^3 any arc of which subtends an angle $\theta \in [0, 2\pi]$ [Fig. 1(a)]. These hard infinitesimally thin curved particles interpolate between the hard infinitesimally thin disk, corresponding to $\theta = 0$, and the hard sphere, corresponding to $\theta = 2\pi$. In the preceding decade, systems of hard spherical caps with $\theta \in [0, \pi]$ were investigated [8]. Their phase behavior features purely entropy-driven cluster columnar and cluster isotropic phases. Since similar, contact-lens-like, colloidal particles have been synthesized [9], these theoretical predictions could be experimentally tested.

Before complementing the investigation on systems of hard spherical caps [8] by investigating systems of hard spherical capsids with $\theta \in (\pi, 2\pi]$, it seems opportune to dedicate the present investigation to the analogous two-dimensional problem: The complete phase behavior of systems of hard infinitesimally thin circular arcs in the two-dimensional Euclidean space \mathbb{R}^2 that subtend an angle $\theta \in [0, 2\pi]$ [Fig. 1(b)]. This class of hard curved particles interpolates between the hard segment, corresponding to $\theta = 0$, and the hard circle, corresponding to $\theta = 2\pi$; it can be divided into the subclass of hard infinitesimally thin minor circular arcs, from $\theta = 0$ up to $\theta = \pi$, and the subclass of hard infinitesimally thin major circular arcs, from $\theta = \pi^+$ up to $\theta = 2\pi$ (Fig. 2).

In addition to the utility of addressing the same type of physical problem across different dimensions, there is another motivation to investigate the complete phase behavior

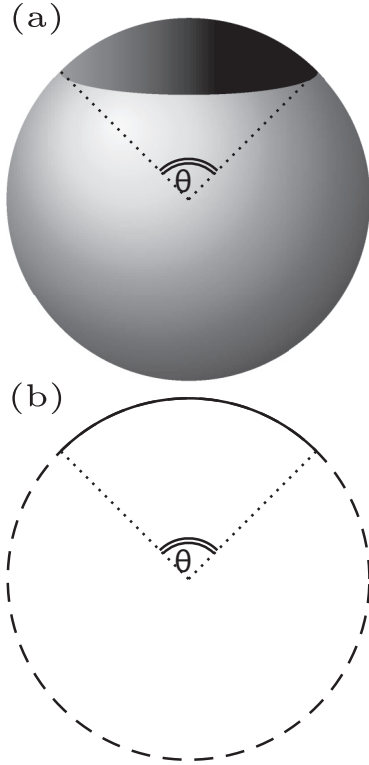


FIG. 1. (a) In three dimensions, given a spherical surface (shaded lighter gray), a spherical cap(sid) (shaded darker gray) is a portion of it any arc of which subtends an angle θ . (b) In two dimensions, given a circumference (dashed line), an arc (solid line) is a portion of it that subtends an angle θ .

of systems of hard infinitesimally thin circular arcs. It is the desire of exploring whether the recently constructed densest known packings of hard infinitesimally thin major circular arcs [10] or suboptimal versions of them can spontaneously form. These densest known packings consist of compact cir-

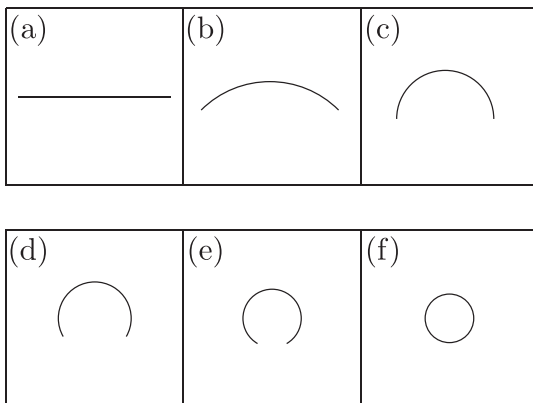


FIG. 2. Examples of circular arcs. They have the same length and different subtended angle θ . Those in the top row are minor: (a) $\theta = 0$, (b) $\theta = \frac{\pi}{2}$, and (c) $\theta = \pi$. Those in the bottom row are major: (d) $\theta = \frac{4}{3}\pi$, (e) $\theta = \frac{5}{3}\pi$, and (f) $\theta = 2\pi$.

cular clusters that comprise [11]

$$n = \left\lceil \frac{2\pi}{\theta - \pi} \right\rceil \quad (1)$$

(counter)clockwise intertwining, hard infinitesimally thin major circular arcs and dispose themselves with their centers of mass at the sites of a triangular lattice [10]. It should be probed whether a similar cluster phase will finally emerge out of a competition with the other phases that systems of hard infinitesimally thin circular arcs form.

To characterize these phases, a set of order parameters and correlation functions is considered (Sec. II A). These structural descriptors are calculated by statistically analyzing the configurations that are saved and stored in the course of isobaric(-isothermal) Monte Carlo numerical simulations [12–14] (Sec. II B). One of the phases that the resulting phase diagram features is that cluster phase. Provided ρ is sufficiently high, it forms in systems of hard infinitesimally thin (quasi)major circular arcs. This phase constitutes the spontaneous, though suboptimal, version of the densest known packings that have been recently determined [10] (Sec. III). While sketching this phase diagram, a few traits of the phases that it features and of the transitions between them emerge that would require as many dedicated theoretical investigations. It is hoped that the present results stimulate these theoretical investigations along with the preparation of colloidal or granular thin-circular-arc-shaped particles and the ensuing experimental investigation of systems of them (Sec. IV).

II. METHODS

A. Order parameters and correlation functions

Certain order parameters and correlation functions are ordinary and prefigurable based on the nonsphericity and (generally¹ D_1) symmetry of the present hard particles and the abundant previous work on systems of hard (non)spherical particles [2].

The most basic correlation function is the positional pair-correlation function which, in a uniform (or treated as if it were such) system of N particles is usually indicated as $g(r)$. It can be defined as

$$g(r) = \frac{1}{N} \left\langle \frac{1}{\rho} \sum_{i=1}^N \sum_{j \neq i}^N \delta(|\mathbf{r}_j - \mathbf{r}_i| - r) \right\rangle, \quad (2)$$

with $\langle \rangle$ signifying a mean over configurations, $\delta(\cdot)$ the usual delta function, and \mathbf{r}_i the position of the centroid of particle i ; presently, this centroid coincides with the vertex of the circular arc i (Fig. 3).

One order parameter that the symmetry of the present hard particles simply suggests is the polar order parameter S_1 . It can be defined as

$$S_1 = \frac{1}{N} \left\langle \left| \sum_{i=1}^N e^{i\varphi_i} \right| \right\rangle = \frac{1}{N} \left\langle \left| \sum_{i=1}^N \hat{\mathbf{u}}_i \right| \right\rangle, \quad (3)$$

with $\hat{\mathbf{u}}_i = (\cos \varphi_i, \sin \varphi_i)$ the unit vector along the symmetry axis of the circular arc i (Fig. 3).

¹Except for $\theta = 2\pi$, in which case it is $O(2)$.

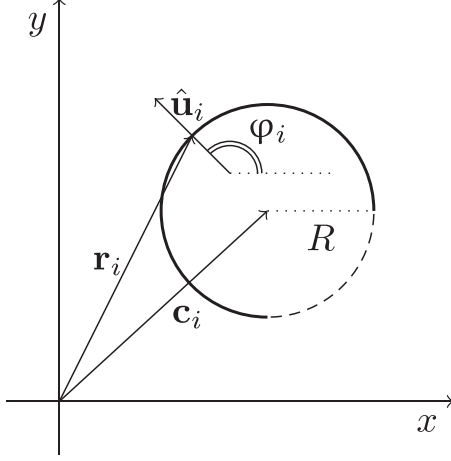


FIG. 3. Example of a circular arc i (solid line) in a Cartesian (x, y) reference frame with several quantities that define its mechanical state and enter the definition of order parameters and correlation functions: \mathbf{r}_i , the vector of the position of its vertex; $\hat{\mathbf{u}}_i$, the unit vector of its orientation, which lies in the direction joining the center of its parent circle with its vertex and forms an angle φ_i with the x axis; and \mathbf{c}_i , the vector of the position of the center of its parent circle (dashed line) whose radius is R .

The nonsphericity of the present hard particles suggests the calculation of the nematic order parameter S_2 . It can be defined as

$$S_2 = \frac{1}{N} \left\langle \left| \sum_{i=1}^N e^{i2\varphi_i} \right| \right\rangle = \left\langle \frac{1}{N} \sum_{i=1}^N [2(\hat{\mathbf{u}}_i \cdot \hat{n})^2 - 1] \right\rangle, \quad (4)$$

with \hat{n} the nematic director, i.e., the direction along which the orientation of a circular arc more probably aligns [15].

The two order parameters S_1 and S_2 would serve to establish whether and of which type a phase possesses orientational order. In actuality, associated with each of these order parameters is an orientational pair-correlation function that provides significantly more information. The two respective correlation functions $\mathcal{G}_1(r)$ and $\mathcal{G}_2(r)$ are defined as

$$\mathcal{G}_1(r) = \left\langle \frac{\sum_{i=1}^N \sum_{j \neq i}^N \delta(|\mathbf{r}_j - \mathbf{r}_i| - r) [\hat{\mathbf{u}}_i(\mathbf{r}_i) \cdot \hat{\mathbf{u}}_j(\mathbf{r}_j)]}{\sum_{i=1}^N \sum_{j \neq i}^N \delta(|\mathbf{r}_j - \mathbf{r}_i| - r)} \right\rangle, \quad (5)$$

$$\mathcal{G}_2(r) = \left\langle \frac{\sum_{i=1}^N \sum_{j \neq i}^N \delta(|\mathbf{r}_j - \mathbf{r}_i| - r) \{2[\hat{\mathbf{u}}_i(\mathbf{r}_i) \cdot \hat{\mathbf{u}}_j(\mathbf{r}_j)]^2 - 1\}}{\sum_{i=1}^N \sum_{j \neq i}^N \delta(|\mathbf{r}_j - \mathbf{r}_i| - r)} \right\rangle. \quad (6)$$

Not only would the values of S_1 and S_2 be obtainable from the $r \rightarrow \infty$ limit of, respectively, $\mathcal{G}_1(r)$ and $\mathcal{G}_2(r)$ but also the calculation of orientational pair-correlation functions allows one to more profoundly characterize the orientational order of a phase. In fact, the possible tendency of two particles to mutually align can be characterized for any distance separating them and the way by which that long-distance limit is approached can be probed.²

²Higher-order orientational pair-correlation functions and their associated order parameters could be considered but, based on the

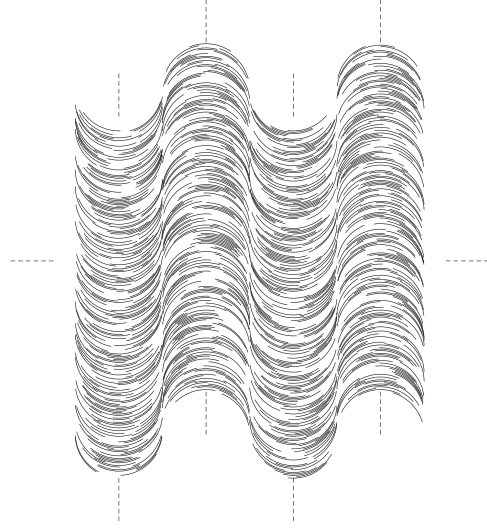


FIG. 4. Schematic illustration of a configuration of an idealized prototypical version of the filamentary phase in a system of hard infinitesimally thin minor circular arcs with, e.g., $\theta = 1$.

The possible formation of anisotropic phases suggests the definition of additional orientational pair-correlation functions whose argument is the interparticle distance vector that is resolved along a certain specific direction. In particular, one can consider the orientational pair-correlation function $\mathcal{G}_{1,\perp}^{\hat{\mathbf{u}}}(r_{\perp})$ defined as

$$\mathcal{G}_{1,\perp}^{\hat{\mathbf{u}}}(r_{\perp}) = \left\langle \frac{\sum_{i=1}^N \sum_{j \neq i}^N \delta(|\mathbf{r}_j - \mathbf{r}_i - (\mathbf{r}_j - \mathbf{r}_i) \cdot \hat{\mathbf{u}}_i \hat{\mathbf{u}}_i| - r_{\perp}) [\hat{\mathbf{u}}_i(\mathbf{r}_i) \cdot \hat{\mathbf{u}}_j(\mathbf{r}_j)]}{\sum_{i=1}^N \sum_{j \neq i}^N \delta(|\mathbf{r}_j - \mathbf{r}_i - (\mathbf{r}_j - \mathbf{r}_i) \cdot \hat{\mathbf{u}}_i \hat{\mathbf{u}}_i| - r_{\perp})} \right\rangle. \quad (7)$$

It probes the polar orientational correlations between two particles separated by a distance vector that is resolved along the direction perpendicular to the orientation of one of them.

The particular nature of the present hard particles and the fact that systems of them may form, in addition to the isotropic and (quasi)nematic³ phases, distinctive phases suggest special order parameters and correlation functions.

The particular nature of the present hard particles suggests probing the positional correlation between a pair of them in terms of the centers of their parent circles. The definition of the corresponding pair-correlation function $G(c)$ parallels that of $g(r)$ in Eq. (2),

$$G(c) = \frac{1}{N} \left\langle \frac{1}{\rho} \sum_{i=1}^N \sum_{j \neq i}^N \delta(|\mathbf{c}_j - \mathbf{c}_i| - c) \right\rangle, \quad (8)$$

experience that was acquired with systems of hard spherical caps [8], those of order 1 and 2 were considered sufficient. In addition, more general orientational pair-correlation functions that depend not only on the modulus but also on the direction of the interparticle distance vector could be profitably considered.

³The prefix (quasi) is added to indicate that, in a two-dimensional system, a proper long-range nematic ordering, like any other proper long-range ordering, would not exist.

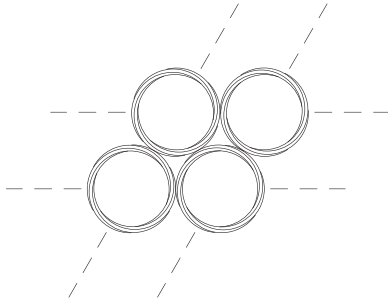


FIG. 5. Schematic illustration of a configuration of an idealized prototypical version of a cluster hexagonal phase in a system of hard infinitesimally thin major circular arcs with, e.g., $\theta = 1.3\pi = 4.084\dots$. Roundish clusters of hard infinitesimally thin major circular arcs dispose themselves with their centers of mass at the sites of a triangular lattice. The hard infinitesimally thin major circular arcs are with, e.g., $\theta = 1.3\pi = 4.084\dots$, so each roundish cluster is composed of a maximum of $n = 6$ of them (see Eq. (1) and [11]). The hard infinitesimally thin major circular arcs are purposely structurally organized in an expanded configuration to aid the appreciation of their (counter)clockwise vortical structural organization. Towards the densest known packings, each roundish cluster progressively contracts and the triangular-lattice spacing consequently decreases up to a point that hard infinitesimally thin major circular arcs essentially are on the same circumference and the triangular-lattice spacing is equal to $2R$.

with \mathbf{c}_i the position of the center of the parent circle of particle i (Fig. 3).⁴

In analogy with the phase behavior of hard spherical caps with $\theta \in [0, \pi]$ [8(b)], systems of hard infinitesimally thin minor circular arcs may form a filamentary phase (Fig. 4). In a filament of this phase, the hard infinitesimally thin minor circular arcs tend to organize on the same semicircumference with the centers of the parent circles that subsequently and randomly file; a single filament is thus polar. Different filaments of this phase may dispose themselves in a row along a direction approximately perpendicular to the filament axis, separated by a distance approximately equal to $2R$ and oriented (anti)parallel to adjacent filaments; the filamentary phase is (more probably) nonpolar. If particularly preceded by a (quasi)nematic phase, the formation of this phase can be revealed by a decrease in the values of S_2 . More generally, its formation can be revealed by the appearance of oscillations in the $\mathcal{G}_{1,\perp}^{\mathbf{u}}(r_{\perp})$ and a sequence of equispaced peaks in the $g(r)$ and $G(c)$.

The structure of the densest known packings of hard infinitesimally thin major arcs [10] suggests a suitably modified hexatic bond-orientational order parameter. These densest known packings and the corresponding cluster hexagonal phase have a two-level structural organization (Fig. 5). On the first level, a maximum of n (see Eq. (1) and [11]) hard infinitesimally thin major circular arcs form roundish clusters that are reminiscent of a vortex. On the second level,

these roundish clusters organize in configurations that are reminiscent of the densest configuration of hard circles [16]. This second-level structural organization suggests a hexatic bond-orientational order parameter ψ_6 . It is defined as

$$\psi_6 = \left\langle \frac{1}{\mathcal{N}} \left| \sum_{i=1}^{\mathcal{N}} \frac{1}{n_{\text{vic}i}} \sum_{j=1}^{n_{\text{vic}i}} e^{i6\varphi_{ij}} \right| \right\rangle, \quad (9)$$

with \mathcal{N} the number of roundish clusters; $n_{\text{vic}i}$ the number of vicinal roundish clusters j of a certain roundish cluster i , defined as those roundish clusters j whose centers of mass are within a prefixed distance from the center of mass of the roundish cluster i ; and φ_{ij} the angle that the fictitious “bond” between the roundish clusters i and j forms with an arbitrary fixed axis. The application of this order parameter naturally presupposes that sufficiently compact and numerous roundish clusters are at least incipient. This can be detected by $G(c)$ via a peak at $c = 0$. Further growth of this peak, together with the growth of the peak at $c = 2R$ and the progressive split of the peak at $c \simeq 4R$, reveals that the processes of formation of roundish clusters and of their hexagonal structural organization are consolidating.

B. Monte Carlo numerical simulations

Systems of hard infinitesimally thin circular arcs were investigated by the Monte Carlo (MC) [12–14] method in the isobaric(-isothermal) (NPT) [13,14] ensemble. The number of particles usually was $N = 600$, although larger values of N were also considered such as $N = 5400$ for various values of θ and occasionally $N = 6400$ in the limit $\theta \rightarrow 0$. The N hard infinitesimally thin circular arcs were placed in an either rectangular or parallelogrammatic variable container. The usual periodic boundary conditions were applied. The pressure P was measured in units of $k_B T \ell^{-2}$, with k_B the Boltzmann constant, T the absolute (thermodynamic) temperature, and $\ell = \theta R$ the length of a circular arc. For any value of θ that was investigated, many values of the dimensionless pressure $P^* = P \ell^2 / (k_B T)$ were considered. For any value of these, the initial configuration was either a (dis)ordered configuration that was constructed *ad hoc* or a configuration that was previously generated in a MC calculation at a nearby value of θ or P^* . From the initial configuration, the MC calculations (sequentially) proceeded. Successive changes were attempted. Each of them was randomly chosen among $2N + 1$ possibilities: With probability $N/(2N + 1)$, a random translation of the centroid of a randomly selected particle; with probability $N/(2N + 1)$, a random rotation of the symmetry axis of a randomly selected particle; and with probability $1/(2N + 1)$, a modification of one randomly selected side of the container. The (pseudo)random number generator that was employed was one that implements the Mersenne Twister mt19937 algorithm [17]. These changes were accepted if no overlap resulted or rejected otherwise. The acceptance of a change in the shape and size of the container was further subject to the Metropolis-like criterion that characterizes the MC method in the NPT ensemble [13,14]. For any specific values of θ and P^* , the maximal amounts of change were adjusted so that 20–30% of each type of change could be accepted; these adjustments were carried out in the course of exploratory MC calculations;

⁴Oriental pair-correlation functions similar to Eqs. (5) and (6) could be defined in terms of the centers of the parent circles, but their calculation was omitted.

the maximal amounts of change were not altered in the course of subsequent MC calculations that were conducted at those specific values of θ and P^* . To improve on the efficiency of the MC calculations, neighbor lists or linked-cell lists were employed (see [14], particularly [14(a)]). In both cases, the operative parameter was $r_{\text{cut}} = 4R \sin(\theta/4)$, which is the minimal distance at which two hard infinitesimally thin circular arcs do not overlap, irrespective of their mutual orientation. In the case of neighbor lists, the list of neighbors of a particle i comprised those particles j whose distance from the centroid of i was smaller than $r_{\text{cut}} + r_{\text{skin}}$; r_{skin} was that distance that had been selected in the course of exploratory MC calculations as the one that provided the largest efficiency. Neighbor lists were automatically updated as soon as $[r_{\text{skin}} - 2d_{\text{max}}]\kappa < r_{\text{cut}}(1 - \kappa)$; d_{max} was the maximum among the particle displacements since the last update of the neighbor lists; κ was the ratio between the new and old values of the length of the modified side of the container. In the case of linked-cell lists, generally rectangular cells were constructed whose minor side was at least equal to r_{cut} so that the largest possible number of cells could be obtained. Linked-cell lists were automatically updated as soon as, following a change in the side of the container, either the minor side of a cell became smaller than r_{cut} and thus a smaller number of cells had to be considered or it became sufficiently larger than r_{cut} to allow for more cells to be considered. For any specific values of θ and P^* , exploratory MC calculations were conducted to decide which type of lists led to the largest efficiency; neighbor (linked-cell) lists were usually more efficient at higher (lower) density, where the particle mobility was relatively small (large). It was also attempted to combine neighbor lists with linked-cell lists but to no avail: Efficiency did not significantly improve with respect to separately considering the sole neighbor lists or linked-cell lists. The MC calculations were organized in cycles, each of these comprising $2N + 1$ attempts of a change. For any specific values of θ and P^* , the MC calculations were subdivided into an equilibration run and a production run. Usually, an equilibration run lasted 10^7 cycles, while the subsequent production run lasted as many cycles. In the course of the production runs, one of every 10^4 configurations was saved and stored for the subsequent statistical analysis. This statistical analysis comprised the calculation of the mean number density $\langle \rho \rangle$, ρ being measured in units ℓ^{-2} so that the dimensionless number density is $\rho^* = \rho \ell^2$ and its mean $\langle \rho^* \rangle = \langle \rho \rangle \ell^2$ and the calculation of the order parameters and correlation functions that are described in Sec. II A; the errors in $\langle \rho^* \rangle$ and in the order parameters were estimated by a habitual blocking method [18].

III. RESULTS

A. Description

By combining the equation of state and the set of order parameters and correlations functions (Sec. II A) and with the aid of the visual inspection of configurations, four (distinctive) phases have been identified. On varying ρ and θ , in addition to (i) a (quasi)nematic phase, systems of hard infinitesimally thin circular arcs can form (ii) a (cluster) isotropic phase where, if ρ is sufficiently high, either filamentous or roundish clusters of

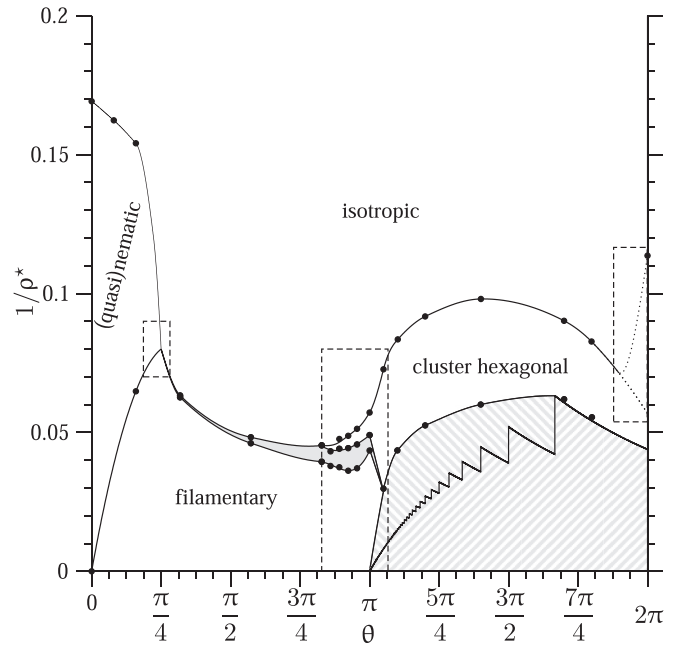


FIG. 6. Phase diagram of systems of hard infinitesimally thin circular arcs in the plane aperture angle θ versus the inverse of the dimensionless number density $1/\rho^*$. Black circles correspond to the original data that have been acquired from the MC numerical simulations, while the solid lines that transverse them are guides to the eye. The gray region on the left is the coexistence region that separates the filamentary phase from either the isotropic phase or the cluster hexagonal phase. The hatched regions on the right are those regions that are effectively or theoretically prohibited as they correspond to values of number density that are higher than the values of number density of the effective or theoretical densest (known) packings: The uppermost monotonic curve that transverse the relevant black circles and delimits the extra region that is hatched with oblique lines from top-left to bottom-right corresponds to the effectively densest packings whose number density has been acquired from the MC numerical simulations; the lower zigzagging curve that delimits the region that is hatched with oblique lines from bottom-left to top-right corresponds to the theoretical densest known packings [10,11]. The two dotted lines towards the hard-circle limits indicate the two possible scenarios of the isotropic-cluster hexagonal phase transition line while approaching that limit. The three dashed rectangles enclose the most delicate regions of the phase diagram.

hard infinitesimally thin circular arcs are recognizable; (iii) a filamentary phase as schematically depicted in Fig. 4; and (iv) a cluster hexagonal phase as schematically depicted in Fig. 5. The regions that the four phases occupy in the θ versus $1/\rho^*$ plane, together with the curves that delimit them, configure the phase diagram in Fig. 6. In describing this phase diagram, it is convenient to subdivide it into four θ -dependent sections: (1) $0 \leq \theta \lesssim \frac{\pi}{4}$, (2) $\frac{\pi}{4} \lesssim \theta < \pi$, (3) $\theta \sim \pi$, and (4) $\theta > \pi$.

1. Section $0 \leq \theta \lesssim \frac{\pi}{4}$

The left-handed side of this section corresponds to the phase behavior of systems of hard segments. The numerical simulation data for this basic reference system were usually interpreted as inconsistent with a second-order isotropic-nematic phase transition that the application of a second-virial

(Onsager [19]) density functional theory would predict [20]. They were usually interpreted as consistent with the existence of an isotropic-(quasi)nematic phase transition of the Berezinskii–Kosterlitz–Thouless [21–24] type [25–27]. One interpretation that essentially maintains both of these, usually mutually exclusive, interpretations was also proposed [28]. In an infinite periodic system, the S-shaped curve of S_2 versus ρ is suggestive of an isotropic-nematic phase transition. In three dimensions, it would be indeed taken as a signature of such a phase transition. In two dimensions, it is instead considered insufficient. This insufficiency is based on assuming that basic analytic results for specific two-dimensional systems [29,30] have to also preclude a proper long-range nematic ordering in a two-dimensional system, even though those analytic results were found inapplicable to a two-dimensional nematic phase that is formed in a realistic system of particles interacting via nonseparable interactions as hard particles are [31]. Based on that paradigm, S_2 of an infinite (thermodynamic) system would be equal to zero at all values of ρ . For this reason, one should turn to explicitly considering $\mathcal{G}_2(r)$ and its long-distance behavior. The latter distinguishes the two phases at either side of a phase transition of the Berezinskii–Kosterlitz–Thouless type: In the isotropic phase, $\mathcal{G}_2(r)$ decays to zero exponentially; in the (quasi)nematic phase, $\mathcal{G}_2(r)$ decays to zero algebraically. Even though past and present numerical simulation data seem to be consistent with this scenario, the limited size of the systems that are considered in these numerical simulations cannot afford to clearly and unambiguously discern the characteristics of the long-distance decay. It is difficult to extrapolate to a very long distance the behavior of a correlation function that is known up to a decade of distance units. Based on this modest distance interval, it is difficult to affirm what the best-fitting function is overall. It seems that, for sufficiently large values of ρ , an algebraic fitting function outperforms an exponential fitting function. However, other fitting functions could perform even better; e.g., a stretched-exponential function fares at least as well as an algebraic function.

Based on these considerations, the attitude of this work is very pragmatic. In analogy to previous works [25,26], $\mathcal{G}_2(r)$ has been fitted to either an exponential or algebraic function. The value of ρ at which the latter fitting function seems to outperform the former fitting function is taken as the value that delimits the isotropic phase and the (quasi)nematic phase. This is done without claiming it as objectively supporting a phase transition of the Berezinskii–Kosterlitz–Thouless type while conceding the present impossibility to more profoundly investigate the nature of the two-dimensional nematic phase and of the transition that separates it from the isotropic phase.

In a system of hard infinitesimally thin minor circular arcs with $\theta = 0.25$, the isotropic and (quasi)nematic phases are the sole phases that have been observed in the interval of values of P that has been presently investigated. Hard infinitesimally thin minor circular arcs with $\theta = 0.5$ are instead sufficiently curved for another, denser and arguably more interesting, phase to succeed the (quasi)nematic phase already in the interval of values of P that has been presently investigated. This phase transition is revealed by a bent in the equation of

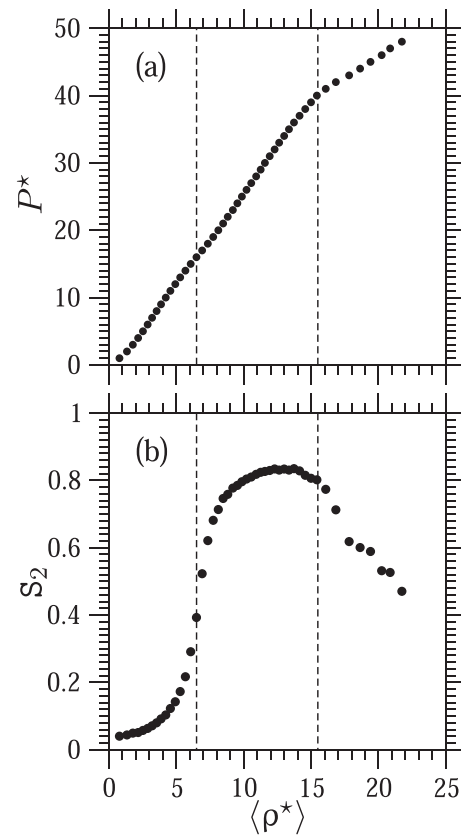


FIG. 7. (a) Equation of state P^* versus $\langle \rho^* \rangle$ and (b) nematic order parameter S_2 versus $\langle \rho^* \rangle$ for a system of hard infinitesimally thin circular arcs with $\theta = 0.5$. The dashed vertical line on the left separates the isotropic phase and the (quasi)nematic phase, while the dashed vertical line on the right separates the (quasi)nematic phase and the filamentary phase.

state and a decrease in the values of S_2 (Fig. 7). These two signs are accompanied by a significant change in the long-distance behavior of $\mathcal{G}_2(r)$. On going from the lower-density phase to the higher-density phase, the long-distance behavior of $\mathcal{G}_2(r)$ seems as if it reverts to that in the isotropic phase: No remnant of a possible algebraic decay remains [Fig. 8(a)]. One can appreciate that the phase that spontaneously forms at larger values of ρ is the filamentary phase [Figs. 8(b)–(d)]. In fact, this phase is characterized by hard infinitesimally thin minor circular arcs tending to organize on the same semi-circumference; in turn, these generated semicircular clusters file to generate filaments; and in turn these filaments tend to mutually organize side by side and up side down [Fig. 8(d)]. Consistently, $\mathcal{G}_{1,\perp}^0(r_\perp)$ exhibits a short-distance oscillatory behavior with a period approximately equal to $2R$ [Fig. 8(e)]. It is conceivable that the filamentary phase also forms in systems of hard infinitesimally thin minor circular arcs with $\theta < 0.5$ at increasingly higher density and pressure than those that have been presently investigated. By the concomitant action of both the isotropic phase at lower ρ and the filamentary phase at higher ρ , the number density interval in which the (quasi)nematic phase exists precipitously contracts as θ increases until this phase disappears at $\theta \simeq \frac{\pi}{4}$.

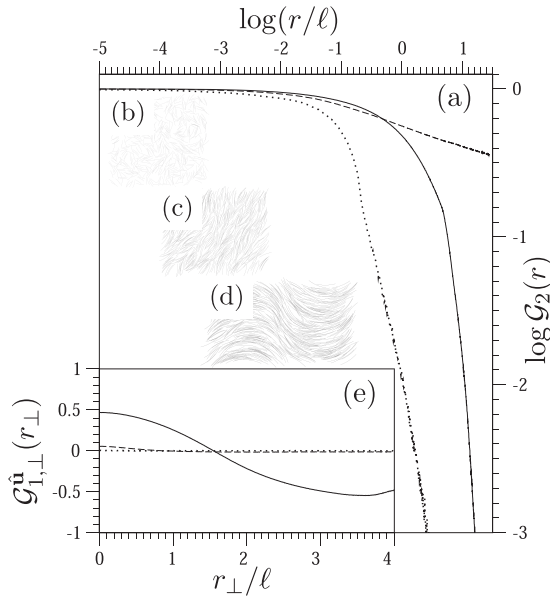


FIG. 8. (a) Orientational pair-correlation function $\mathcal{G}_2(r)$ in the isotropic phase at $P^* = 10$ (dotted line), (quasi)nematic phase at $P^* = 35$ (dashed line), and filamentary phase at $P^* = 45$ (solid line). Also shown are images of a configuration in the (b) isotropic phase at $P^* = 10$, (c) (quasi)nematic phase at $P^* = 35$, and (d) filamentary phase at $P^* = 45$. (e) Orientational pair-correlation function $\mathcal{G}_{1,\perp}^u(r_\perp)$ in the isotropic phase at $P^* = 10$ (dotted line), (quasi)nematic phase at $P^* = 35$ (dashed line), and filamentary phase at $P^* = 45$ (solid line).

2. Section $\frac{\pi}{4} \lesssim \theta < \pi$

In this section the isotropic and filamentary are the sole phases that are observed. These two phases are separated by a first-order phase transition whose strength increases with increasing θ . This is revealed by the behavior of the equation of state [Fig. 9(a)]. The S_2 concurs to reveal this phase transition: S_2 exhibits a surge in correspondence to the values of ρ at which the phase transition occurs; the values that this order parameter takes in the filamentary phase are significantly smaller than those typical of a (quasi)nematic phase [Fig. 9(b)]. In fact, in an idealized prototypical filamentary phase as schematically depicted in Fig. 4, the S_2 would take a value equal to $\frac{\sin(\theta-\pi)}{\theta-\pi}$. The structural differences that occur on going from the isotropic phase to the filamentary phase are revealed by the various pair-correlation functions (Fig. 10). In particular, $G(c)$ peaks at $c = 2R$ and $4R$ [cf. Figs. 10(a) and 10(b)], while $\mathcal{G}_{1,\perp}^u(r_\perp)$ becomes oscillatory with a period equal to $4R$ [cf. Figs. 10(e) and 10(f)]. On increasing θ , as the transition to the filamentary phase is approached, the isotropic phase passes from being ordinary to exhibiting clusters. These clusters are made of hard infinitesimally thin circular arcs that tend to organize on the same semicircumference and then file to generate filaments that are of varying length, degree of ramification, and tortuosity [inset in Fig. 10(c)]. The progressive straightening of the equation of state is a symptom of the formation of these “supraparticular” structures that precurse a proper filamentary phase. On increasing θ , in the same filamentary phase, the filaments tend to be more tortuous and it is increasingly more frequent to observe ramifications and

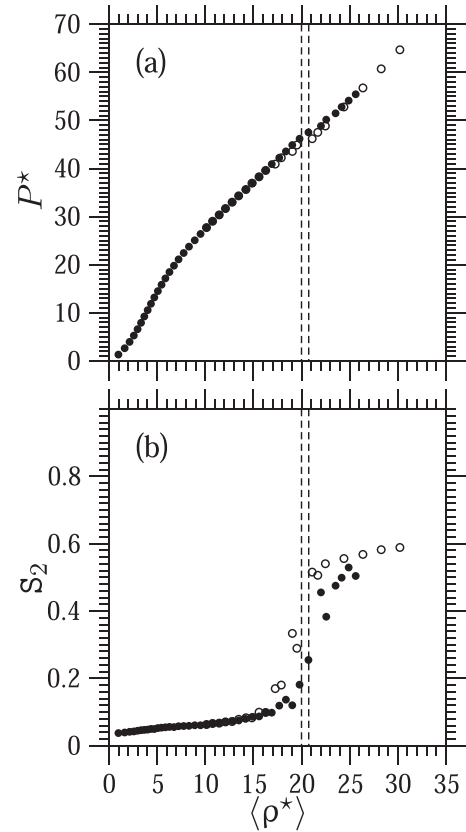


FIG. 9. (a) Equation of state P^* versus $\langle \rho^* \rangle$ and (b) nematic order parameter S_2 versus $\langle \rho^* \rangle$ for a system of hard infinitesimally thin circular arcs with $\theta = 1.8$. In both panels, closed circles correspond to data that were obtained by progressively compressing the system from an initial dilute and disordered configuration, while open circles correspond to data that were obtained by progressively decompressing the system from an initial filamentary configuration like that schematically depicted in Fig. 4. The two dashed vertical lines separate the isotropic phase and the filamentary phase.

ruptures. These ramifications and ruptures are provoked by hard infinitesimally thin circular arcs that tend to dispose in an antiparallel configuration [inset in Fig. 10(d)].

3. Section $\theta \sim \pi$

In this section, a new, arguably most interesting, phase appears in between the isotropic phase and the filamentary phase: the cluster hexagonal phase. In the isotropic phase, the tendency that filamentous clusters have to break and close up increases up to conducting to the formation of roundish clusters. This occurs up to a point that the roundish clusters become sufficiently compact and numerous and their number sufficiently large to organize in a triangular lattice. The formation of this cluster hexagonal phase, which prevents the spontaneous formation of the filamentary phase, can be revealed by examining the equation of state: It corresponds to a tenuous surge in its graph that is recognizable at values of $\rho^* \simeq 20$ [Fig. 11(a)]. While S_2 is unable to reveal this phase transition [Fig. 11(b)], better evidence of a transition between the isotropic phase and the cluster hexagonal phase is nonetheless acquired by examining the dependence of ψ_6 on ρ : This

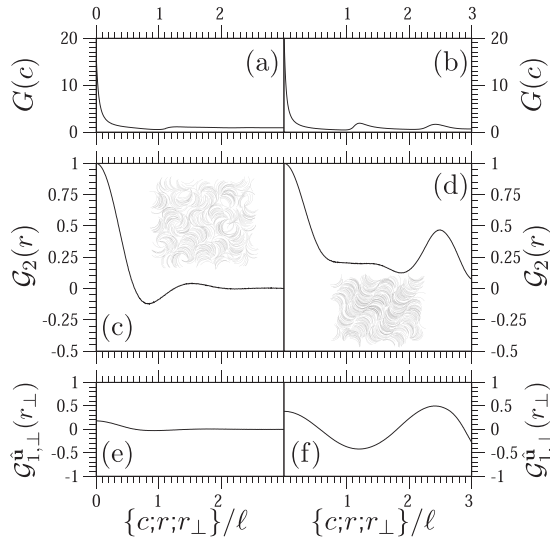


FIG. 10. Shown for a system of hard infinitesimally thin circular arcs with $\theta = 1.8$ in the isotropic phase at $P^* = 40$ and in the filamentary phase at $P^* = 53$, respectively, are (a) and (b) the positional pair-correlation function $G(c)$, (c) and (d) the orientational pair-correlation function $G_2(r)$, and (e) and (f) the orientational pair-correlation function $G_{1,\perp}^u(r_\perp)$. The inset in (c) is an image of a configuration in the isotropic phase at $P^* = 40$, while the inset in (d) is an image of a configuration in the filamentary phase at $P^* = 53$.

order parameter exhibits a clear surge in correspondence to the isotropic-cluster hexagonal phase transition [Fig. 11(c)]. The S_2 can instead distinguish between the cluster hexagonal phase and the filamentary phase: Since the roundish clusters are overall isotropic, S_2 (effectively) vanishes in the cluster hexagonal phase as it does in the isotropic phase; since the structural units of the filamentary phase are formed by a progressively smaller number of hard infinitesimally thin minor circular arcs as $\theta \rightarrow \pi$, S_2 is increasingly significantly larger than zero in the filamentary phase [Fig. 11(b)]. The two cluster phases are separated by a first-order phase transition. The structural differences among the three phases are revealed by the various pair-correlation functions and evidenced by the corresponding images of a configuration (Fig. 12). Based on these images, one can note the similarity between the structures of the isotropic phase and of the cluster hexagonal phase which contrast with the structure of the filamentary phase. This (dis)similarity among the three phases is reflected in the graphs of the various pair-correlation functions (Fig. 12).

4. Section $\theta > \pi$

The fact that θ surpasses the intermediate value of π is very consequential. It was already observed that two hard infinitesimally thin major circular arcs that are disposed on top of one another cannot be superposed; they can only be superposed if they are suitably rotated with respect to one another in a way that, once it is exactly replicated n (see Eq. (1) and [11]) minus two times, conduces to the formation of those compact circular clusters that characterize the corresponding densest known packings [10]. This fact significantly destabilizes the filamentary phase with respect to the cluster hexagonal phase: The former phase precipitously disappears, leaving the latter

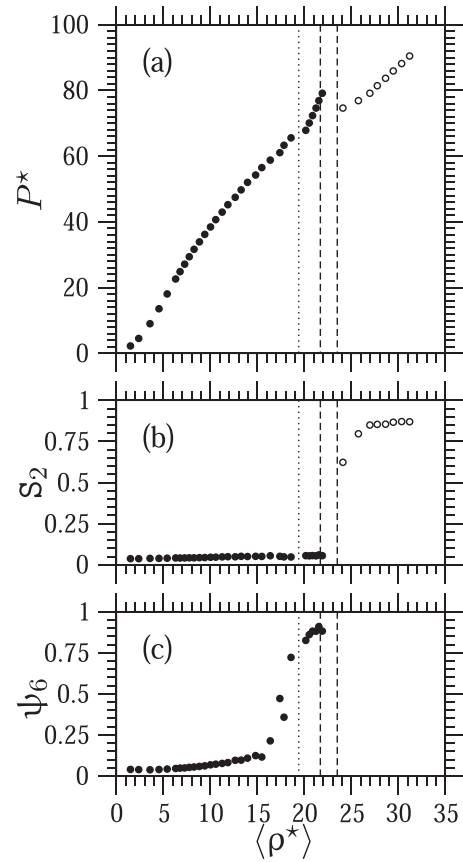


FIG. 11. (a) Equation of state P^* versus $\langle \rho^* \rangle$, (b) nematic order parameter S_2 versus $\langle \rho^* \rangle$, and (c) hexatic order parameter ψ_6 versus $\langle \rho^* \rangle$ for a system of hard infinitesimally thin circular arcs with $\theta = 3$. In (a) and (b) closed circles correspond to data that were obtained by progressively compressing the system from an initial dilute and disordered configuration, while open circles correspond to data that were obtained by progressively decompressing the system from an initial filamentary configuration like that schematically depicted in Fig. 4. In the three panels, the vertical dotted line separates the isotropic phase and the cluster hexagonal phase, while the two vertical dashed lines separate the cluster hexagonal phase and the filamentary phase.

phase as the sole observable phase at sufficiently high ρ . The cluster hexagonal phase is separated from the isotropic phase by a transition whose weakness presently makes it impossible to assess whether it is either (more probably) first order or second order. This phase transition is revealed by a visually recognizable change in the graph of the equation of state [Fig. 13(a)]. This change may be made clearer by plotting the effective packing fraction $\eta^* = \frac{\rho\pi R^2}{\pi/(2\sqrt{3})}$ with respect to the inverse compressibility factor $\zeta = \frac{\rho^*}{P^*}$ [Fig. 13(b)]. One further revealer of the formation of a cluster hexagonal phase is again ψ_6 : It exhibits a surge in correspondence to $\langle \rho^* \rangle \simeq 12$, the value of $\langle \rho^* \rangle$ at which the isotropic-cluster-hexagonal phase transition occurs [Fig. 14(a)]. In addition, the form of $g(r)$ and $G(c)$ passes from being fluidlike [Figs. 14(b) and 14(c)] to being crystalline-like [Figs. 14(d) and 14(e)].

In the graphical representation of Fig. 13(b), one can observe that the cluster-hexagonal-phase branch is, to a good

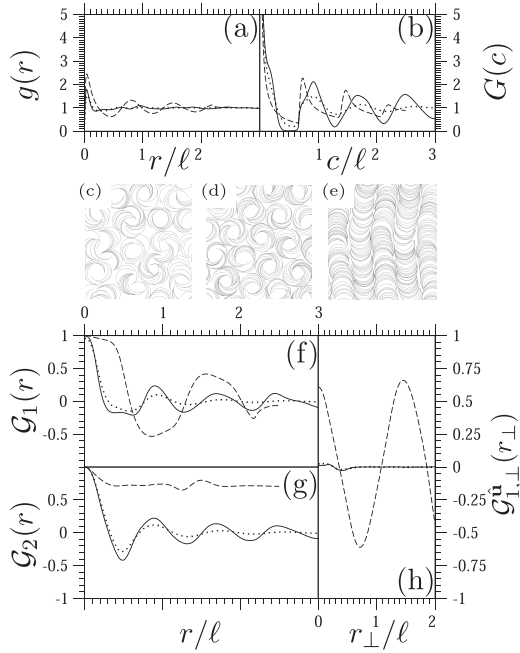


FIG. 12. Shown for a system of hard infinitesimally thin circular arcs with $\theta = 3$ in the isotropic phase at $P^* = 25$, the cluster hexagonal phase at $P^* = 34$, and the filamentary phase at $P^* = 34$ are (a) the positional pair-correlation function $g(r)$; (b) the positional pair-correlation function $G(c)$; (c)–(e) image of a configuration in the (c) isotropic phase, (d) cluster hexagonal phase, and (e) filamentary phase; (f) the orientational pair-correlation function $\mathcal{G}_1(r)$; (g) the orientational pair-correlation function $\mathcal{G}_2(r)$; and (h) the orientational pair-correlation function $\mathcal{G}_{1,\perp}^0(r_\perp)$. In (a), (b), and (f)–(h), the dotted, solid, and dashed lines represent the isotropic, cluster hexagonal, and filamentary phases, respectively.

approximation, linear. This is consistent with the applicability, also to the present case, of a suitably adapted version of the free-volume theory [32]. This theory is known to provide a good description and interpretation of the equation of state of a dense solid phase in a system of hard particles [32,33]. In an equilibrium system of hard circles (disks), the linear extrapolation of the high-density solid-branch curve would intersect the ordinate axis at a value equal to 1. The linear extrapolation of the high-density solid-branch curve in a system of hard infinitesimally thin major circular arcs with $\theta = 1.1\pi = 3.455\dots$ intersects the ordinate axis at a value approximately equal to 6.5 [Fig. 13(b)]. This value corresponds to the mean value $\langle n \rangle$ of the hard infinitesimally thin major circular arcs with $\theta = 1.1\pi = 3.455\dots$ per roundish cluster. This is confirmed by a more direct calculation of $\langle n \rangle$. It ensues from the calculation of the probability distribution \mathcal{P} of the number n of hard infinitesimally thin major circular arcs per roundish cluster: $\mathcal{P}(n)$ [Fig. 15(a)]. The value of $\langle n \rangle$ increases with $\langle \rho^* \rangle$ in the isotropic phase until it flatly levels up as the system enters the cluster hexagonal phase [Fig. 15(b)]. The limit value $\langle n \rangle \simeq 6.5$ in the cluster hexagonal phase is smaller than $n = 19$ (see Eq. (1)) and [11]) [10]. This means that the cluster hexagonal phase that spontaneously forms from the isotropic phase is a suboptimal version of these densest known packings. This is comprehensible as the

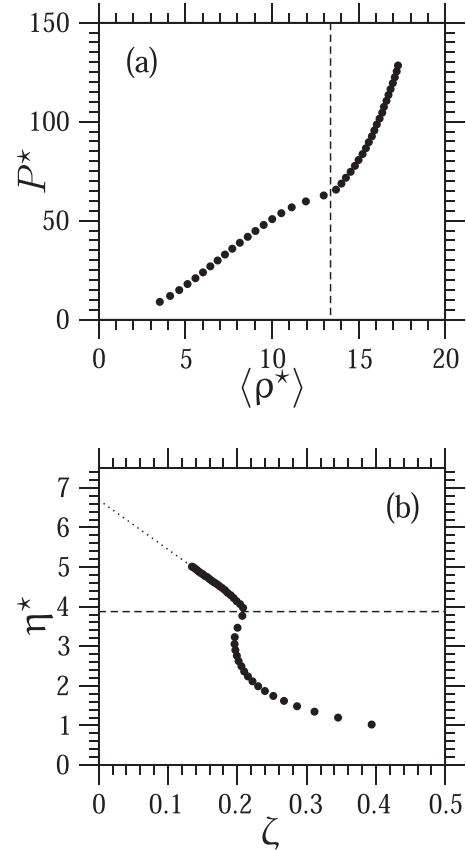


FIG. 13. Equation of state (a) in the representation P^* versus $\langle \rho^* \rangle$ and (b) in the representation η^* versus ζ for a system of hard infinitesimally thin circular arcs with $\theta = 1.1\pi = 3.455\dots$. In (a) the vertical dashed line and in (b) the horizontal dashed line separate the isotropic phase and the cluster hexagonal phase; in (b) the dotted line is a linear fit extrapolation of the higher-density part of the solid-phase branch.

phase transition occurs at a value of $\langle \rho^* \rangle \simeq 12$ that is still relatively small [Fig. 15(b)]. Yet the subsequent constancy of $\langle n \rangle$ with $\langle \rho^* \rangle$ [Fig. 15(b)] raises two questions as to whether the densest known packings could ever spontaneously form on progressive compression and whether the cluster hexagonal phase that spontaneously forms from the isotropic phase could ever be an equilibrium phase. The importance and relevance of these questions also emerge from investigating systems of hard infinitesimally thin major circular arcs with a larger value of θ . In these cases, more than one cluster hexagonal phase branch can be observed; these are separated by what would seem to be a first-order phase transition [Fig. 16(a)]. Such a discontinuous phase behavior can be also appreciated by examining the evolution of ρ^* in the course of a Monte Carlo numerical simulation: An abrupt jump in the values of ρ^* is frequently observed [Fig. 16(b)]. This is due to the roundish clusters that are progressively reorganizing in such a way that they incorporate, on average, more constituting hard infinitesimally thin circular arcs: In correspondence to the rise in the values of ρ^* there is a momentary fall in the values of ψ_6 ; this suggests a momentary reorganization of the system that allows the incorporation of more hard infinitesimally thin circular arcs into the same roundish cluster(s) [Fig. 16(c)]. The

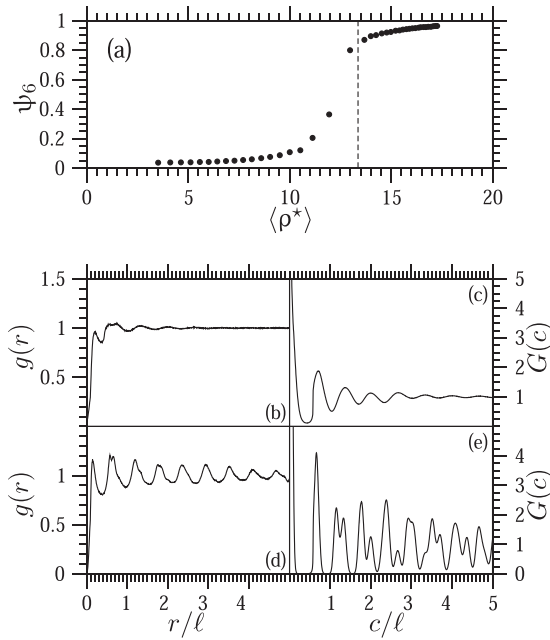


FIG. 14. Shown for a system of hard infinitesimally thin circular arcs with $\theta = 1.1\pi = 3.455\dots$ are (a) the order parameter ψ_6 as a function of number density $\langle\rho^*\rangle$, where the vertical dashed line separates the isotropic phase and the cluster hexagonal phase, and (b)–(e) the pair-correlation functions $g(r)$ and $G(c)$ in (b) and (c) the isotropic phase at $P^* = 56.7$ and (d) and (e) in the cluster hexagonal phase at $P^* = 128.4$.

lower-density branch directly forms from the isotropic phase [Fig. 16(a)]. If pressure is sufficiently high, then it transforms into the higher-density branch after many MC cycles (Fig. 16). From that value of pressure, the higher-density branch can be continued up to higher pressure and down to lower pressure [Fig. 16(a)]. One may assess the lower-density branch in Fig. 16(a) as an enduring metastable branch. However, the same assessment is applicable to the unique branch that is observed in Fig. 13 and to the higher-density branch in Fig. 16(a) with respect to other, hypothesizable, even higher-density branches that insufficiently lengthy MC numerical simulations prevent from observing. Continuous incorporation and release of hard infinitesimally thin circular arcs into or from roundish clusters are necessary to spontaneously attain and maintain an equilibrium $\mathcal{P}(n)$. In a cluster hexagonal phase, it is conceivable that the mechanisms of incorporation and release become increasingly less effective as ρ increases. Based on Figs. 13, 15, and 16, it is presently unclear how an equilibrium cluster hexagonal phase should proceed towards the densest known packing limit: either continuously, via a gradual modification of $\mathcal{P}(n)$, or discontinuously, via a sequence of isostructural first-order phase transitions, each phase at either side of the phase transition being a cluster hexagonal phase with its own $\mathcal{P}(n)$. The discontinuous behavior that is observed may well be an artificial effect due to the finite size of the systems that are considered in the MC numerical simulations, which is further exacerbated by the (always looming) insufficiency of their duration.

On progressive compression from the isotropic phase, the capability that hard infinitesimally thin major circular arcs

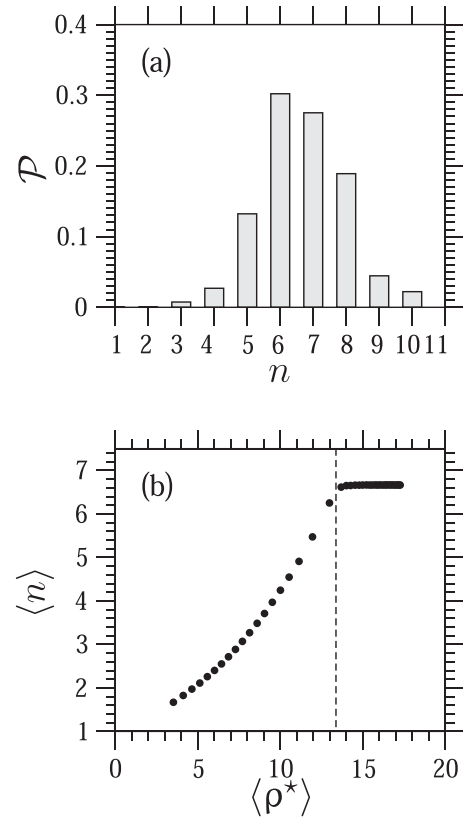


FIG. 15. (a) Probability distribution function \mathcal{P} of the number n of hard infinitesimally thin circular arcs per roundish cluster for a system of hard infinitesimally thin circular arcs with $\theta = 1.1\pi = 3.455\dots$ at $P^* = 128.4$. (b) Mean value $\langle n \rangle$ of the number of hard infinitesimally thin circular arcs per roundish cluster as a function of $\langle\rho^*\rangle$ for a system of hard infinitesimally thin circular arcs with $\theta = 1.1\pi = 3.455\dots$. The vertical dashed line separates the isotropic phase and the cluster hexagonal phase.

have to intertwine in roundish clusters persists up to values of θ almost equal to 2π : For a value of θ as large as $1.9\pi = 5.969\dots$ a vast majority of dimers are observed. This capability should deteriorate as the value of θ is further increased: In the very close neighborhood of $\theta = 2\pi$, a more even mixture of monomers and dimers is expected, with the former progressively becoming more abundant as the hard-circle limit is approached. In the hard-circle limit, the system is clearly formed by single hard circles. However, it is probable that this limit should be considered as a singular limit. This hypothesis relies on the densest known packings being formed by dimers that dispose themselves with their centers of mass at the sites of a triangular lattice for any value of $\theta < 2\pi$ [10]. In the thermodynamic limit at very high density, the stablest structures should correspond to these densest known packings for any value of $\theta < 2\pi$ [10].

B. Discussion

In discussing the phase diagram that has been described, there are several comparisons to be made and connections to be established with previous works.

Section 1 resembles the phase diagram of a generalized planar rotor spin system on a square lattice. In this system,

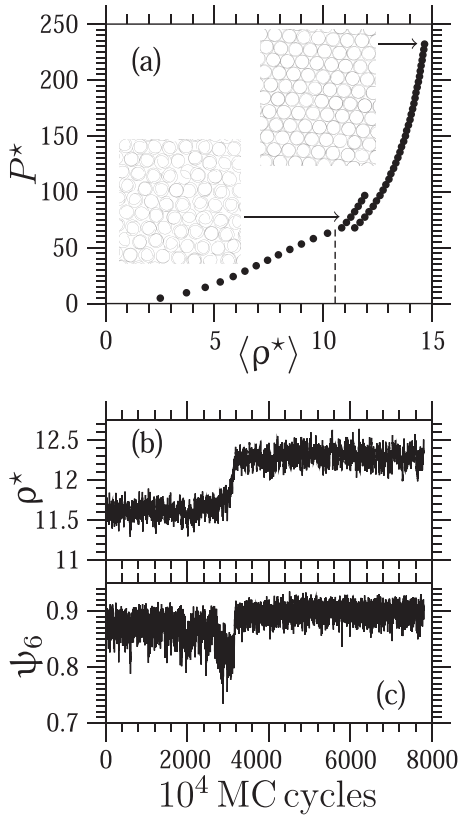


FIG. 16. Shown for a system of hard infinitesimally thin circular arcs with $\theta = 1.4\pi = 4.398\dots$ are (a) the equation of state P^* versus $\langle \rho^* \rangle$ (note that there are two cluster-hexagonal branches), where the vertical dashed line separates the isotropic phase and the lower-density cluster-hexagonal phase, the inset on the bottom left is an image of a configuration taken at $P^* = 77.4$ in the lower-density cluster-hexagonal branch, and the inset on the top right is an image of a configuration taken at $P^* = 232.1$ in the higher-density cluster-hexagonal branch; (b) the evolution of the number density ρ^* at $P^* = 77.4$ as a function of MC cycles; and (c) the evolution of the order parameter ψ_6 at $P^* = 77.4$ as a function of MC cycles.

the interaction of a spin i with its nearest-neighbor spin j comprises the (ferromagnetic or) polar term, proportional to $\cos(\varphi_j - \varphi_i)$, and the (generalized) nematic term, proportional to $\cos[q(\varphi_j - \varphi_i)]$, with $q = 2, 3, 4$ [34–37]. This resemblance is made once the low-density isotropic (high-density filamentary) phase in the present off-lattice systems is associated with the high-temperature paramagnetic (low-temperature ferromagnetic) phase in those on-lattice systems. In both types of systems, a (quasi)nematic phase exists in between the other two respective phases. Its stability interval diminishes as either θ increases or the polar term proportional to $\cos(\varphi_j - \varphi_i)$ prevails, respectively. However, this resemblance may be solely qualitative and a possible correspondence between the two types of systems may immediately end. Even though sharing the same rotational symmetry, investigations on on-lattice systems of spins interacting with a potential energy U of the form

$$U = -a_1 \cos(\varphi_j - \varphi_i) - a_q \cos[q(\varphi_j - \varphi_i)],$$

TABLE I. First four coefficients of the Fourier series of the excluded area between two hard infinitesimally thin circular arcs that subtend an angle θ ; note that the coefficients are in units of the coefficient a_2 .

θ	a_1/a_2	a_2/a_2	a_3/a_2	a_4/a_2
0	0	1	0	0.2
0.11285	-0.000762	1	-0.000754	0.198
0.56608	-0.0214	1	-0.0196	0.158
1.14391	-0.107	1	-0.0755	0.0873

with $q \geq 2$, have shown that the resulting phase diagrams can significantly depend on q [36]. It is presumable that the same conclusion holds when other, more general, expressions for the potential energy of the form

$$U = - \sum_{q \geq 1} a_q \cos[q(\varphi_j - \varphi_i)]$$

are considered [38]. The excluded area could be considered as the quantity in a two-dimensional off-lattice nonthermal model that plays a role analogous to the potential energy in a two-dimensional on-lattice thermal model. In fact, there has been an investigation of a system of spins on a square lattice interacting with a potential energy of the same form as the excluded area between two discorectangles [39]. If one adapted this exercise to the present case, one would have to calculate the excluded area between two hard infinitesimally thin minor circular arcs. The first four terms of the Fourier series expansion of this excluded area (Table I) would indicate that the effect of progressively curving hard segments into hard infinitesimally thin minor circular arcs would be to generally make the effective interactions more isotropic. These effective interactions would be essentially classifiable as a composition of an (antiferromagnetic or) antipolar term with a nematic term (Table I). This would not be entirely compatible with the observation of a filamentary phase which, although globally nonpolar, is locally polar. The passage from an on-lattice model to an off-lattice model does not seem to be that straightforward: If even maintaining the particles constrained on a lattice and changing a sole term proportional to $\cos[q(\varphi_j - \varphi_i)]$ produces qualitatively different phase diagrams, then results that may be valid for an on-lattice system may not apply, especially in low dimensions, to a supposedly related off-lattice system. Not only are the centroids of the hard infinitesimally thin circular arcs not constrained on a lattice, but the interaction between two of them is also non-separable. This significantly adds to debilitating a possible association between the filamentary phase in a system of hard infinitesimally thin minor circular arcs and the ferromagnetic phase in a system of generalized planar rotor spins: In fact, even leaving aside the positional structure of the filamentary phase, its orientational pair-correlation functions are significantly more complicated than the simple algebraically and monotonically decaying pair-correlation functions in the ferromagnetic phase.

The filamentary phase is the same phase that was observed in numerical simulations on systems of hard bow-shaped particles formed by three suitably disposed hard segments

[40(a)]. In that work, this phase was referred to as a modulated nematic phase. In a subsequent work that attempted to reproduce these numerical simulation data with second-virial (Onsager [19]) density-functional theory analytic calculations, this phase was interpreted as a splay-bend nematic phase [40(b)]. Irrespective of whether it could be qualified as generically modulated or particularly a splay-bend phase, it is actually the application of the adjective *nematic* to this phase that is unconvincing. One constitutive feature of a nematic phase is its positional uniformity. The filamentary phase, even in those versions that are very rippled with ramifications, ruptures, and tortuosity, is not positionally uniform; e.g., the probability density to find a particle intrafilament is not the same as that to find a particle interfilament. One more constitutive feature of a nematic phase is its fluidity. One would expect that particles travel along the modulation in a modulated nematic phase as fast as they do along the nematic director in an ordinary nematic phase. This is what happens in the screwlike nematic phase that forms in systems of helical particles [41]. Preliminary results on the mechanism of diffusion in the filamentary phase that forms in systems of hard infinitesimally thin circular arcs indicate that this is not the case [42]: Hard infinitesimally thin circular arcs intrude from one filament into an adjacent filament in a steplike manner while retaining their orientation and rapidly return to the original filament or advance to the subsequent filament, a mechanism of diffusion that is reminiscent of the one operative in a smectic-A phase [43]. These considerations are consistent with what was ultimately observed in systems of hard arched particles in three dimensions. Initially, numerical simulations and experiments on systems of hard or colloidal arched particles claimed that these systems form a splay-bend nematic phase [44(a,b)]. Subsequently, this conclusion was rectified: That modulated phase is not positionally uniform; it is not nematic but smecticlike [44(c)].

Rather, the concavity and polarity of the present hard particles induce the recognition of another resemblance, between the cluster isotropic phase and the filamentary phase that are observed in section 2 of the present phase diagram and the “living polymeric” phase that was observed in systems of dipolar hard circles (disks) [45]. In both present and previous systems, filaments or chains form which are tortuous and occasionally ramify and close up to produce roundish clusters or irregular rings.

Sections 1 and 2 of the phase diagram of systems of hard infinitesimally thin circular arcs constitute (nothing but) the two-dimensional version of the phase diagram of systems of hard spherical caps with subtended angle $\theta \in [0, \pi]$ [8]. In particular, the present filamentary phase is (nothing but) the two-dimensional version of that cluster columnar phase that was observed in three-dimensional systems of hard spherical caps. Consistently to its lower dimension, the filamentary phase is subject to stronger fluctuations that should conduce to a more extensive tortuosity as well as to more ramifications and ruptures. Yet the same autoassembly phenomenology is essentially observed in both two and three dimensions. In particular, it causes the isotropic phase to exhibit, at sufficiently high ρ , the formation of clusters that progressively pass from being filamentous or lacy to being roundish or globular as θ increases. The principal difference between what is observed

in two dimensions and what is observed in three dimensions is the capability of the two-dimensional roundish clusters to organize in a triangular lattice, i.e., the formation of a cluster hexagonal phase in two dimensions.

Though already incipient in section 3, this cluster hexagonal phase completely characterizes section 4 of the phase diagram of Fig. 6. Consistently with the recent determination of the corresponding densest known packings [10], it constitutes the truly new phase that is observed in the present work. It forms in two dimensions, while in three dimensions an analogous phase has not been observed and will probably be not observable. It forms due to the capability that hard infinitesimally thin particularly major, circular arcs have to intertwine without intersecting. This capability cannot be retained on going from two to three dimensions.

Similarly to what has already been commented apropos of the phase behavior of systems of hard spherical caps [8], the autoassembly phenomenology that is observed in systems of hard infinitesimally thin circular arcs resembles what is observed in molecular systems that form micelles [46,47]: These supramolecular structural units can be cylindrical or globular, which can then autoassemble to form a variety of complex phases including columnar and crystalline phases [46,47]. There, at the origin of the complex phase behavior, are complex molecules that interact between them via complicated attractive and repulsive intermolecular interactions. Here, this complex phase behavior occurs in systems of relatively simple hard particles and thus is purely entropy driven.

IV. CONCLUSION AND PERSPECTIVE

This work consists in an investigation on the phase behavior of systems of hard infinitesimally thin circular arcs in the two-dimensional Euclidean space \mathbb{R}^2 . Depending on the subtended angle θ and the number density ρ , several purely entropy-driven phases have been observed in the course of Monte Carlo numerical simulations [12–14].

Leaving aside the (quasi)nematic phase that is solely observed for sufficiently small values of θ and at intermediate values of ρ , more interesting are the other phases that have been observed. The isotropic phase is one such example: Provided ρ is sufficiently high, it becomes no ordinary in that it exhibits clusters which pass from being filamentous to being roundish as θ progressively increases. Provided ρ is even higher, these two types of clusters produce a filamentary phase for $\theta \lesssim \pi$ and a hexagonal phase for $\theta \gtrsim \pi$, respectively. Both these phases are characterized by a supraparticular structural organization: The actual structural units are formed by a number of suitably disposed hard particles. Particularly interesting is the cluster hexagonal phase. It offers examples of (soft) porous crystalloid materials (if a view is naturally taken in the direction that is perpendicular to \mathbb{R}^2) [48] whose porosity could be regulated by compression. The autoassembly phenomenology in systems of hard infinitesimally thin circular arcs, as well as that in systems of hard spherical caps [8], interestingly resembles that which occurs in micellizing molecular systems [46,47].

Despite the extensive Monte Carlo numerical simulations, there are several issues that still need clarification. Leaving aside the persistent issue of the nature of the nematic phase

in a realistic two-dimensional system [31], it is the structure of the three cluster phases that would require a more detailed characterization. This should center on a detailed statistical analysis of the shape and size of respective clusters. Specifically in systems of hard infinitesimally thin minor circular arcs, it should address the persistence length of the filaments and the number of their ramifications and ruptures.⁵ Specifically in systems of hard infinitesimally thin major circular arcs, it should ascertain whether, on progressive compression, a single hexagonal phase forms or multiple hexagonal phases

form in the (long) way towards the corresponding densest known packings [10]. The clarification of these pending issues requires consideration of systems of a significantly larger size and more improved computational resources and techniques than those presently available. Under these conditions, it would be very beneficial to have experimental systems of colloidal or granular thin-circular-arc-shaped particles [49]. It could be used to first test the present predictions on the complete phase behavior and then address and aid the resolution of those pending issues.

⁵It is not clear whether these ramifications and ruptures should be considered as defects or are instead inherent to the very nature of these phases.

ACKNOWLEDGMENT

The authors acknowledge support from the Government of Spain under Grant No. FIS2017-86007-C3-1-P.

- [1] See, e.g., P. M. Chaikin and T. C. Lubensky, *Principles of Condensed Matter Physics* (Cambridge University Press, Cambridge, 1995).
- [2] See, e.g., S. Torquato, *J. Chem. Phys.* **149**, 020901 (2018).
- [3] See, e.g., *The Plastically Crystalline State: Orientationally-Disordered Crystals*, edited by J. N. Sherwood (Wiley, Chichester, 1979).
- [4] See, e.g., L. M. Blinov, *Structure and Properties of Liquid Crystals* (Springer, Dordrecht, 2011).
- [5] L. Mederos, E. Velasco, and Y. Martínez-Ratón, *J. Phys.: Condens. Matter* **26**, 463101 (2014).
- [6] M. P. Allen, *Mol. Phys.* **117**, 2391 (2019).
- [7] See, e.g., C. Avendaño and F. A. Escobedo, *Curr. Opin. Colloid Interface Sci.* **30**, 62 (2017).
- [8] (a) G. Cinacchi and J. S. van Duijneveldt, *J. Phys. Chem. Lett.* **1**, 787 (2010); (b) G. Cinacchi, *J. Chem. Phys.* **139**, 124908 (2013); (c) G. Cinacchi and A. Tani, *ibid.* **141**, 154901 (2014).
- [9] S. Sacanna, M. Korpics, K. Rodriguez, L. Colón-Meléndez, S.-H. Kim, D. J. Pine, and G.-R. Yi, *Nat. Commun.* **4**, 1688 (2013); K. V. Edmond, T. W. P. Jacobson, J. S. Oh, G.-R. Yi, A. D. Hollingsworth, S. Sacanna, and D. J. Pine, *Soft Matter* **17**, 6176 (2021).
- [10] J. P. Ramírez González and G. Cinacchi, *Phys. Rev. E* **102**, 042903 (2020).
- [11] Here, $[x]$ indicates the strict floor function of the real variable x . The adjective *strict* is used to signify that this floor function returns $x - 1$ and not x for $x \in \mathbb{N}$, while it behaves as an ordinary floor function for $x \notin \mathbb{N}$.
- [12] N. Metropolis, A. W. Rosenbluth, M. N. Rosenbluth, A. N. Teller, and E. Teller, *J. Chem. Phys.* **21**, 1087 (1953).
- [13] W. W. Wood, *J. Chem. Phys.* **48**, 415 (1968); **52**, 729 (1970).
- [14] See, e.g., (a) M. P. Allen and D. J. Tildesley, *Computer Simulation of Liquids* (Clarendon, Oxford (1987); (b) W. Krauth, *Statistical Mechanics: Algorithms and Computations* (Oxford University Press, Oxford, 2006).
- [15] J. Vieillard-Baron, *Mol. Phys.* **28**, 809 (1974). This work actually introduced the method, based on ordinary linear algebra, to calculate S_2 and \hat{n} for a system of hard nonspherical particles in three dimensions. The method is, *mutatis mutandis*, the same in a system of hard noncircular particles in two dimensions.
- [16] See, e.g., P. Brass, W. O. J. Moser, and J. Pach, *Research Problems in Discrete Geometry* (Springer, New York, 2005).
- [17] M. Matsumoto and T. Nishimura, *ACM Trans. Model. Comput. Simul.* **8**, 3 (1998).
- [18] H. Flyvbjerg and H. G. Petersen, *J. Chem. Phys.* **91**, 461 (1989); consult also M. Jonsson, *Phys. Rev. E* **98**, 043304 (2018).
- [19] L. Onsager, *Ann. N.Y. Acad. Sci.* **51**, 627 (1949).
- [20] R. F. Kayser and H. J. Raveché, *Phys. Rev. A* **17**, 2067 (1978).
- [21] V. L. Berezinskii, *Zh. Eksp. Teor. Fiz.* **59**, 907 (1971) [*Sov. JETP* **32**, 493 (1971)]; *Zh. Eksp. Teor. Fiz.* **61**, 1144 (1972) [*Sov. JETP* **34**, 610 (1972)]; *Nizkotemperaturnye svoistva dvumernykh sistem s nepreryvnoi gruppoi simmetrii*, Ph.D. thesis, Landau Institute for Theoretical Physics, Moscow, 1971; *Nizkotemperaturnye Svoistva Dvumernykh Sistem s Nepreryvnoi Gruppoi Simmetrii* (Fizmatlit, Moscow, 2007).
- [22] J. M. Kosterlitz and D. J. Thouless, *J. Phys. C* **5**, L124 (1972); **6**, 1181 (1973); J. M. Kosterlitz, *ibid.* **7**, 1046 (1974).
- [23] J. M. Kosterlitz, *Rep. Prog. Phys.* **79**, 026001 (2016).
- [24] V. N. Ryzhov, E. E. Tareyeva, Y. D. Fomin, and E. N. Tsiok, *Usp. Fiz. Nauk.* **187**, 921 (2017) [*Phys. Usp.* **60**, 857 (2017)].
- [25] D. Frenkel and R. Eppenga, *Phys. Rev. A* **31**, 1776 (1985).
- [26] M. D. Khandkar and M. Barma, *Phys. Rev. E* **72**, 051717 (2005).
- [27] R. L. C. Vink, *Eur. Phys. J. B* **72**, 225 (2009).
- [28] A. Chrzanowska, *Acta Phys. Pol. B* **36**, 3163 (2005).
- [29] N. D. Mermin and H. Wagner, *Phys. Rev. Lett.* **17**, 1133 (1967).
- [30] N. D. Mermin, *Phys. Rev.* **176**, 250 (1968).
- [31] J. P. Straley, *Phys. Rev. A* **4**, 675 (1971).
- [32] J. G. Kirkwood, *J. Chem. Phys.* **18**, 380 (1950); W. W. Wood, *ibid.* **20**, 1334 (1952); Z. W. Salsburg and W. W. Wood, *ibid.* **37**, 798 (1962); F. H. Stillinger and Z. W. Salsburg, *J. Stat. Phys.* **1**, 179 (1969).
- [33] A. Donev, S. Torquato, and F. H. Stillinger, *Phys. Rev. E* **71**, 011105 (2005).
- [34] D. H. Lee and G. Grinstein, *Phys. Rev. Lett.* **55**, 541 (1985).
- [35] D. B. Carpenter and J. T. Chalker, *J. Phys.: Condens. Matter* **1**, 4907 (1989).
- [36] F. C. Poderoso, J. J. Arenzon, and Y. Levin, *Phys. Rev. Lett.* **106**, 067202 (2011); G. A. Canova, Y. Levin, and J. J. Arenzon, *Phys. Rev. E* **89**, 012126 (2014); **94**, 032140 (2016).

- [37] D. M. Hübscher and S. Wessel, *Phys. Rev. E* **87**, 062112 (2013).
- [38] In this respect, consult M. Žukovič and G. Kalagov, *Phys. Rev. E* **96**, 022158 (2017); **97**, 052101 (2018); M. Žukovič, *Phys. Lett. A* **382**, 2618 (2018).
- [39] H. Chamati and S. Romano, *Phys. Rev. E* **77**, 051704 (2008).
- [40] (a) R. Tavarone, P. Charbonneau, and H. Stark, *J. Chem. Phys.* **143**, 114505 (2015); (b) P. Karbowniczek, *ibid.* **148**, 136101 (2018).
- [41] E. Barry, Z. Hensel, Z. Dogic, M. Shribak, and R. Oldenbourg, *Phys. Rev. Lett.* **96**, 018305 (2006); H. B. Kolli, E. Frezza, G. Cinacchi, A. Ferrarini, A. Giacometti, and T. S. Hudson, *J. Chem. Phys.* **140**, 081101 (2014); G. Cinacchi, A. M. Pintus, and A. Tani, *ibid.* **145**, 134903 (2016).
- [42] J. P. Ramírez González and G. Cinacchi (unpublished).
- [43] M. P. Lettinga and E. Grelet, *Phys. Rev. Lett.* **99**, 197802 (2007); G. Cinacchi and L. De Gaetani, *Phys. Rev. E* **79**, 011706 (2009).
- [44] (a) M. Chiappini, T. Drwenski, R. van Roij, and M. Dijkstra, *Phys. Rev. Lett.* **123**, 068001 (2019); (b) C. Fernández-Rico, M. Chiappini, T. Yanagishima, H. de Sousa, D. G. A. L. Aarts, M. Dijkstra, and R. P. A. Dullens, *Science* **369**, 950 (2020); (c) M. Chiappini, and M. Dijkstra, *Nat. Commun.* **12**, 2157 (2021).
- [45] J. M. Caillol and J. J. Weis, *Mol. Phys.* **113**, 2487 (2015).
- [46] See, e.g., J. N. Israelachvili, *Intermolecular and Surface Forces* (Academic, New York, 2011).
- [47] Other systems for which a certain resemblance could be recognized are colloidal systems that are formed by Janus colloidal particles; see, e.g., J. S. Oh, S. Lee, S. C. Glotzer, G.-R. Yi, and D. J. Pine, *Nat. Commun.* **10**, 3936 (2019).
- [48] See, e.g., A. G. Slater and A. I. Cooper, *Science* **348**, aaa8075 (2015).
- [49] One possibility could be systems of colloidal particles that suitably generalized those that have been prepared and investigated by P. Y. Wang and T. G. Mason, *J. Am. Chem. Soc.* **137**, 15308 (2015).